Future Technology
Open Access Journal
ISSN 2832-0379

May 2026| Volume 05 | Issue 02 | Pages 221-227

Journal homepage: https://fupubco.com/futech

https://doi.org/10.55670/fpll.futech.5.2.21

Future Publishing LLC

Article

The synergetic effect of in-situ TiB_2 and ex-situ Al_2O_3 in Al-Si binary alloys for the enhancement of wear properties

Adityaprasad Sahoo[1], Sandeep Kumar Sahoo[1]*, Jogendra Majhi[1], Himansu Sekhar Dash[2], Ashok Kumar Pradhan[2]

[1]Department of Metallurgical and Materials Engineering, Indira Gandhi Institute of Technology, Sarang, Odisha, India
[2]Department of Production Engineering, Indira Gandhi Institute of Technology, Sarang, Odisha, India

ARTICLE INFO

Article history:
Received 06 November 2025
Received in revised form
10 February 2026
Accepted 09 March 2026

Keywords:
Hybrid composites, TiB_2, Al_2O_3, Stir casting, Wear

*Corresponding author
Email address:
sandeep.talcher@gmail.com

DOI: 10.55670/fpll.futech.5.2.21

ABSTRACT

In metal matrix composites (MMCs), non-metallic or inter-metallic phases are commonly introduced into a metal or an alloy in a required proportion with an aim to develop a new material that possesses attractive engineering properties. Aluminium matrix composites (AMCs) have been known for their high strength-to-weight ratio, and these are utilized to meet specific requirements in the field of various automotive and aerospace applications. In this study, the hypoeutectic and hypereutectic Al-Si composites have been fabricated through two step stir casting process. TiB_2 incorporation has been facilitated by an exothermic reaction between the molten metal and halide salts (K_2TiF_6 and KBF_4), leading to the in-situ formation of the reinforcement. To develop hybrid composites, Al_2O_3 particles were further added to the melt. The resulting microstructures were analysed using scanning electron microscopy. The presence of Al_2O_3 and TiB_2 phases was confirmed by X-ray Diffraction (XRD). The composites were also evaluated for hardness, density, and dry sliding wear behaviour. The results indicate that the wear rate decreases with increasing TiB_2 content, whereas this improvement is restricted to the addition of 1 wt. % Al_2O_3. Higher applied loads resulted in increased wear rates. Density values of the composites have been found to increase marginally with higher reinforcement content. Hardness improves with Al_2O_3 addition up to 1 wt. %; and a further addition of 2 wt. % causes a decrease in hardness due to particle agglomeration.

1. Introduction

Composite fabrication is a promising technique for enhancing the properties of traditional materials to meet the demands of various engineering sectors, owing to its significant design flexibility. Aluminium, the most abundant metal in the earth's crust, and its alloys often top the list of materials that fulfil the requirements of aerospace and electric vehicle sectors due to their high specific strength, resulting in weight reduction, which ultimately improves fuel efficiency and performance. Excellent castability of Al-Si alloys, along with their superior wear and corrosion resistance, thermal conductivity, and a low coefficient of thermal expansion, makes them the preferred choice of their class. These low-density aluminium alloys can also accommodate ceramic particles like Al_2O_3 and TiB_2 as reinforcement to enhance their mechanical and wear properties [1,2]. A wide range of investigations on hypoeutectic Al-Si alloy-based composites suggest that eutectic and hypereutectic alloys can be a good replacement for cast iron counterparts, especially in engine parts. The deciding factor in modifying the mechanical properties of these alloys is the morphology and distribution of constituent phases, such as primary and eutectic silicon, and thus, the role of the reinforcement particles becomes more critical in this regard. Reinforcements such as Al_2O_3 and TiB_2 can provide nucleation sites for grain refinement. Further, in-situ formation of TiB_2 provides a clean interface between the matrix and reinforcement, which has the ability to enhance mechanical as well as tribological properties of the composites [3–5]. The objective of the present work is to synthesize and characterize hybrid composites of Al-Si hypo and hypereutectic alloys reinforced with in-situ TiB_2 (2, 5 wt. %) and ex-situ Al_2O_3 (1, 2 wt. %) and study the effect of reinforcements (TiB_2 and Al_2O_3) and Si content on the microstructure and wear characteristics of the composites.

2. Materials and methods

2.1 Composite fabrication

Aluminium (commercially pure) was melted in a pit-type laboratory furnace in a graphite crucible, and then an Al-50Si master alloy was introduced into the molten aluminium at 800°C and held for 30 minutes to ensure complete dissolution. The calculated amounts (as per stoichiometric calculations considering 20% loss) of halide salts K_2TiF_6 (250µm) and KBF_4 (30µm) were preheated at 200°C for 2 hours in a drying oven to remove moisture and then cooled to room temperature. Then the salts were wrapped in Al foils and put into the melt held at 800°C. The halide salts were used to in situ form TiB_2 in the molten matrix via salt-metal reaction. The dross was removed by decanting after 30 minutes (completion of the reaction), and Al_2O_3 powder was introduced to synthesize Al-Si-TiB_2/Al_2O_3 hybrid composite [6–8]. The stirring rod (graphite rod coated with zirconia paste) was immersed and fixed at a depth of about 2/3rd of the molten metal. Intermittent stirring for 30 seconds was carried out at 10-minute intervals at a stirring speed of 100-200 rpm to ensure proper distribution of the reinforcement particles. Degassing was carried out using hexachloroethane before pouring. The molten composite was poured into a cast iron mould, preheated at 450°C to cast the required composites [9, 10].

2.2 Microstructure analysis

Samples for microstructure were prepared from the cast composites by metallographic specimen preparation practice by using a low-speed precision cutter, a belt grinder, and a twin disc table-top polisher. The low-speed saw is generally employed as a versatile precision cutter for sample preparation, allowing user-controlled sectioning that minimizes the risk of mechanical and thermal damage to materials, while providing parallel, smooth sample surfaces for efficient further processing. A freshly prepared Keller's reagent (2.5 vol. % HNO_3, 1.5 vol. % HCl, 1 vol. % HF & 95 vol. % H_2O) was utilized for etching (7-10 seconds). Prepared samples were observed under a Scanning Electron Microscope to study the microstructure of the composites of different compositions.

2.3 X-ray diffraction study

X-Ray Diffraction study of the samples (2mm thick) was carried out to find out the presence of the in-situ synthesized TiB_2 particles and other phases in the cast composites [10].

2.4 Wear properties

The cast composites were machined to form required-sized pins (30mm height, 10mm diameter) for the pin-on-disc (Magnum Engineers) wear test. Composite pins were subjected to sliding against a steel (EN31) disc (8mm thickness and 100mm diameter) in dry conditions under different applied loads at a velocity of 1m/s for a 1000m distance in ambient temperature, with reference to ASTM G99 standard, to study the wear behavior of the composites [11]. Surface roughness was maintained at 0.31 to 0.78 µm for pins and 0.02 to 0.06 µm for the disc [12].

2.5 Density and hardness studies

A Micro Vickers hardness tester, utilizing a square-based diamond pyramid indenter, was used to measure the hardness of the composite specimens under an applied load of 1 kgf for 15 seconds. Additionally, the density of the Al-Si-TiB_2/Al_2O_3 composites was determined using a digital balance with an integrated density measurement kit (Mettler-Toledo) by using Archimedes' principle.

3. Results and discussion

The chemical composition of the cast composites is presented in Table 1.

Table 1. Chemical composition of the cast composites

Sl. No.	Composite Code	Chemical Composition
1	A20	Al-11.8wt.%Si-2wt.%TiB_2
2	A21	Al-11.8wt.%Si-2wt.%TiB_2-1wt.% Al_2O_3
3	A22	Al-11.8wt.%Si-2wt.%TiB_2-2wt.% Al_2O_3
4	A50	Al-11.8wt.%Si-5wt.%TiB_2
5	A51	Al-11.8wt.%Si-5wt.%TiB_2-1wt.% Al_2O_3
6	A52	Al-11.8wt.%Si-5wt.%TiB_2-2wt.% Al_2O_3
7	B20	Al-13.5wt.%Si-2wt.%TiB_2
8	B21	Al-13.5wt.%Si-2wt.%TiB_2-1wt.% Al_2O_3
9	B22	Al-13.5wt.%Si-2wt.%TiB_2-2wt.% Al_2O_3
10	B50	Al-13.5wt.%Si-5wt.%TiB_2
11	B51	Al-13.5wt.%Si-5wt.%TiB_2-1wt.% Al_2O_3
12	B52	Al-13.5wt.%Si-5wt.%TiB_2-2wt.% Al_2O_3

3.1 Microstructure analysis

The scanning electron micrographs of the composites are shown in Figure1. Composites of hypoeutectic alloy composition (Al-11.8Si) typically display a primary α-Al phase, which is surrounded by a needle-like eutectic structure. However, Figure 1 (b, e) show more fine structures with the incorporation of Al_2O_3 into the composite [13, 14]. But further increase in Al_2O_3 from 1wt. % to 2 wt. % does not have a proportionate effect with respect to grain refinement (Figure 1c, 1f).

Figure 1 clearly shows that the bright, needle-like eutectic silicon phase becomes more refined as the TiB_2 content increases from 2 wt. % to 5 wt. %. Small amounts of primary silicon particles are also observed in some microstructures due to non-equilibrium solidification and minor compositional variations. The addition of 1 wt. % Al_2O_3 contributes to grain refinement, as the fine ceramic particles serve as heterogeneous nucleation sites [13, 14]. However, increasing the Al_2O_3 content to 2 wt. % does not result in any further noticeable improvement in the microstructure. It is due to the fact that a higher amount of Al2O3 (2 wt. %) leads to promoting agglomeration of the particles.

Al-13.5Si alloy composites (hyper eutectic) are shown in Figure 1 (g-l). Fine dendrites of the α-Al phase, along with rod-like Si, are observed in the microstructure. With increasing TiB_2 content, these Si rods become smaller and slimmer. For a fixed amount of Al_2O_3, the microstructure of the composites of both compositions (hypoeutectic and hypereutectic) illustrates grain refinement with increasing TiB_2 content. This observation is supported by the findings of A. Mandal et al. [7]. Microstructural analysis indicates that both types of ceramic particles are effective in refining the grain structure of Al-Si alloys.

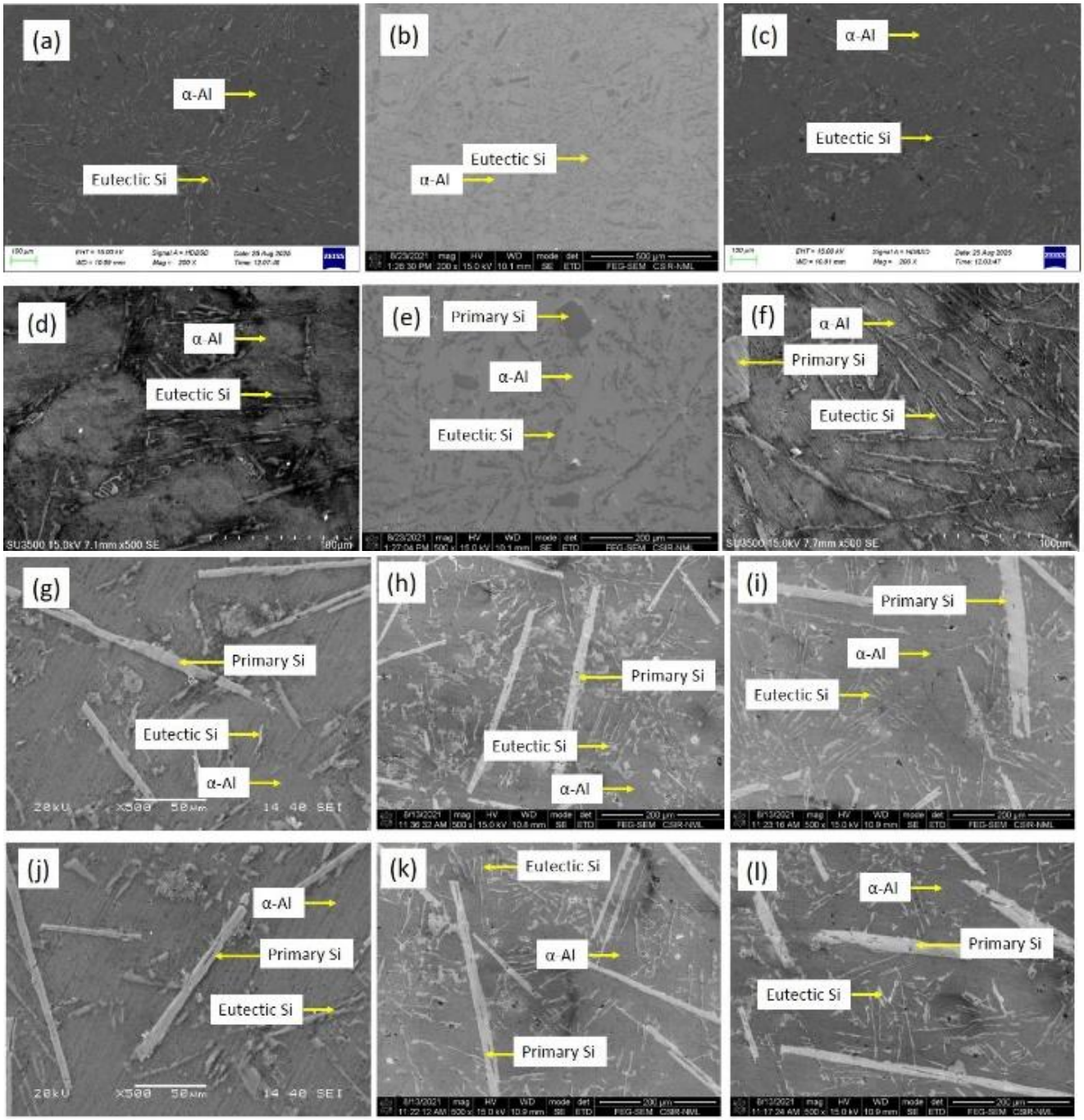

Figure 1. SEM of Al-11.8Si alloy with (a) $2TiB_2$ [A20], (b) $2TiB_2$ & $1Al_2O_3$ [A21] and (c) $2TiB_2$ & $2Al_2O_3$ [A22] at 200X mag. (d) $5TiB_2$ [A50], (e) $5TiB_2$ & $1Al_2O_3$ [A51], (f) $5TiB_2$ & $2Al_2O_3$ [A52] and SEM of Al-13.5Si-alloy with (g) $2TiB_2$ [B20], (h) $2TiB_2$ & $1Al_2O_3$ [B21] and (i) $2TiB_2$ & $2Al_2O_3$ [B22] (j) $5TiB_2$ [B50], (k) $5TiB_2$ & $1Al_2O_3$ [B51], (l) $5TiB_2$ & $2Al_2O_3$ [B52] at 500X magnification.

3.2 EDS Analysis

Figure 2 (a) spectrum 003 of Al-11.8Si-$2TiB_2$ reveals the tallest peak for silicon, adjacent to a relatively smaller peak for aluminium, along with tiny peaks for titanium and boron. The conventional SEM-EDS has intrinsic limitations in accurately quantifying very light elements such as boron due to low X-ray energy (~183 eV), absorption effects, and background uncertainty. In the present work, the boron signal obtained from EDS was therefore interpreted only qualitatively to confirm its presence. This states that the halide salts (K_2TiF_6 and KBF_4) undergo decomposition into Ti and B via a salt-metal reaction during stir-casting.

TiB_2 forms preferentially over Al_3Ti and AlB_2 because the ΔG of TiB_2 formation is more negative within the operating temperature range [15]. The thermodynamic calculations for the reaction between K_2TiF_6 and KBF_4 in molten aluminium reveal that the Gibbs free energy change (ΔG) for the synthesis of TiB_2 is more negative than that for the formation of Al_3Ti and AlB_2 in the temperature range of 430-930°C. Consequently, TiB_2 is formed instead of Al_3Ti and AlB_2. The Gibbs free energy for Al_3Ti formation increases with temperature, but TiB_2 is more stable and therefore forms only at high temperatures. The thermodynamic data suggest that TiB_2 formation temperature is in the range of 750 - 900°C [15,

16]. The presence of TiB_2 is also confirmed by XRD analysis. Spectrum 2 in Figure 2 (b) also shows Ti and B peaks along with Al in Al-13.5-Si-5TiB_2.

3.3 X-ray diffraction studies

X-Ray Diffraction study of composites containing 11.8 and 13.5 wt. % Si are shown in Figure 3. The plots reveal prominent peaks for aluminium, as these are Al-based alloys, along with smaller peaks for silicon. Tiny Al_2O_3 and TiB_2 peaks are also seen. TiB_2 peaks are clearly visible in composites with 5 wt. % TiB_2. This suggests that salt-metal reaction yields TiB_2, but at a lower amount of TiB_2 content, these particles are completely engulfed by the Aluminium (Al) or Silicon (Si) phases for producing nucleation sites [17].

3.4 Wear studies

Figure 4 (a-c) presents the wear rate of Al-11.8Si-TiB_2 composites under a constant load, whereas the Al_2O_3 content is varied. Initially, increasing the Al2O3 content reduces the wear rate, indicating improved wear resistance. However, when the Al_2O_3 content increases beyond 1 wt. %, the wear rate starts to rise, suggesting that excessive Al_2O_3 (above 1wt.%) adversely affects the composite's wear performance. Figure 4 (d-f) also shows a similar trend in wear rate. The 2TiB_2 line is found to be above the 5TiB_2 line. This indicates that the greater the TiB_2 content, the lower the wear rate. This is due to the fact that TiB_2 is a good grain refiner in Al-Si alloys, and lower wear is caused by the fine grain structure of the composites. The in-situ TiB_2 particles in the composites are mostly free of defects and maintain their structure during sliding. Additionally, the uniform distribution of these TiB_2 particles contributes to Orowan strengthening [18–20].

In Figure 5a, the black line represents the dislocation line in the Orowan model process, and L symbolizes the interparticle gap. The dislocation line moves forward and forms a loop as it passes two particles. As a result, a new structure known as a dispersion strengthening structure (Figure 5b) is created. This dispersion accounts for improved mechanical properties of cast Al-Si alloys with particle reinforcements [21]. Though Al_2O_3 promotes heterogeneous nucleation, its role as a grain refiner is restricted to 1 wt. %, beyond this limit, agglomeration begins, and its efficiency decreases. Improved hardness values resulting from the incorporation of these ceramic particles also corroborate the wear test results.

3.5 Worn surfaces studies

Figure 6 shows the microstructure of the worn surface of Al-13.5 wt. % Si-5 wt. % TiB_2 composites. Microstructural analysis of the worn surface shows that, under identical wear test conditions, the sample with 1 wt. % Al_2O_3 shows fine grooves and cracks (Figure 5a) whereas composite with 2 wt. % Al_2O_3 shows deeper grooves and more voids and cracks (Figure 5b). This reveals that as the amount of Al_2O_3 increases, wear increases. This occurs because increasing the amount of Al_2O_3 leads to clustering of the particles, and these brittle particles are being cut off during the course of sliding, to maintain the relative motion between the disc and the composite pin [5, 22–24].

3.6 Density and hardness studies

Table 2 shows the theoretical (rule of mixture) density of the composites compared with experimentally measured density. The porosity was found to be within 1%, indicating the good quality of the castings obtained in the stir-casting process.

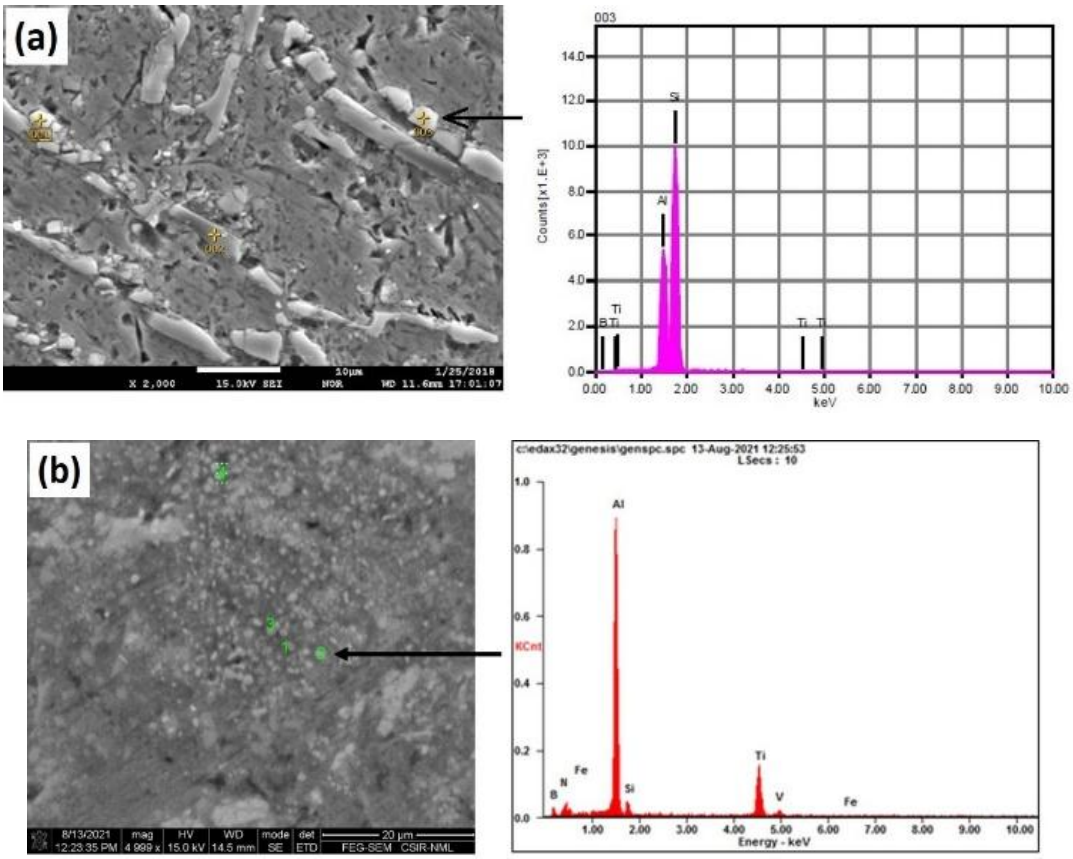

Figure 2. Energy dispersive X-ray spectroscopy (EDS) analysis of sample (a) A20 (Al-11.8Si-2TiB_2), (b) B20 (Al-13.5-Si-5TiB_2).

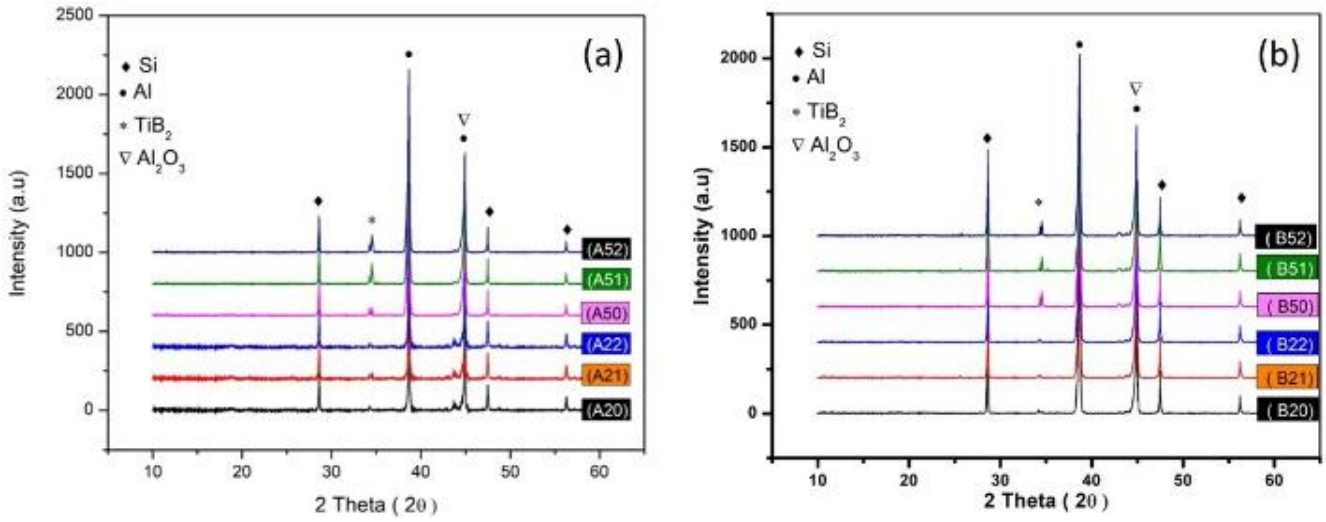

Figure 3. XRD plots of composite samples containing (a) 11.8wt. %Si (b) 13.5wt.%Si

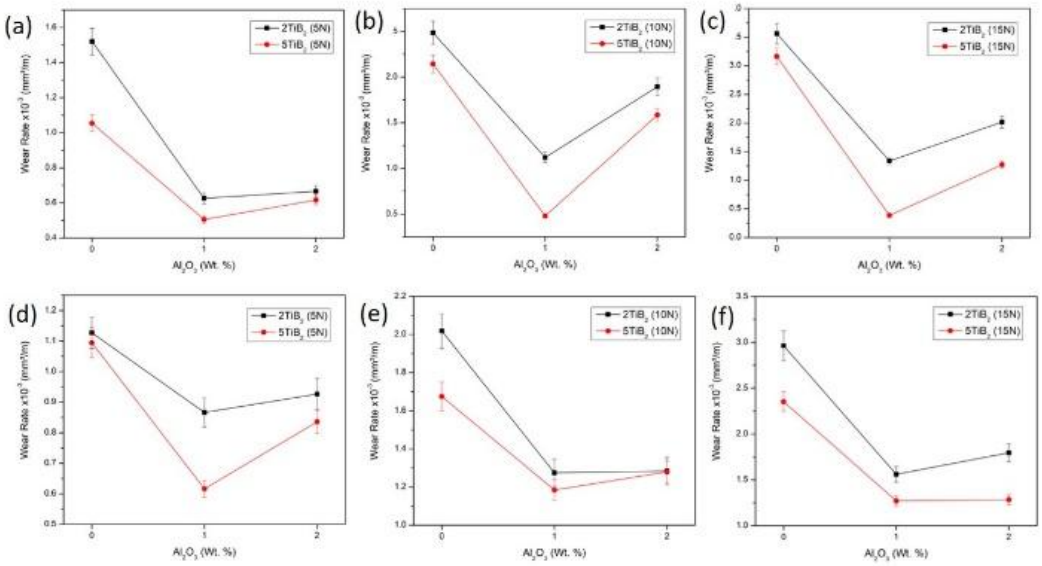

Figure 4. Wear rate of Al-11.8 wt. % Si composites Vs wt. % Al_2O_3 at (a) 5N, (b) 10 N and (c) 15N Loads and Wear rate of Al-13.5 wt. % Si composites Vs wt. % Al_2O_3 at (d) 5N, (e) 10 N and (f) 15N Loads

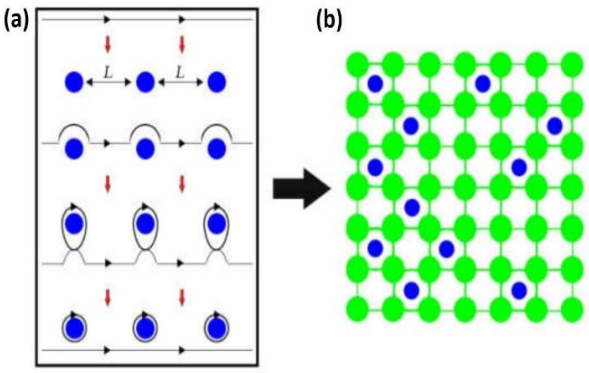

Figure 5. Strengthening mechanisms (a) OROWAN model (b) Dispersion strengthening [21]

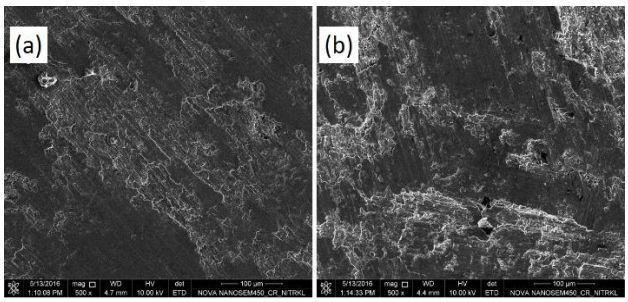

Figure 6. Scanning electron microscopy of the worn surface of (a) B51 (b) B52 composites

Table 2. Density of the cast composites

Sl. No.	Composite Code	Theoretical Density	Experimental Density	Porosity (%)
1	A20	2.69274	2.675	0.66
2	A21	2.70564	2.689	0.62
3	A22	2.71854	2.694	0.90
4	A50	2.74734	2.721	0.96
5	A51	2.76024	2.738	0.81
6	A52	2.77314	2.751	0.80
7	B20	2.68645	2.664	0.84
8	B21	2.69935	2.678	0.79
9	B22	2.71225	2.691	0.78
10	B50	2.74105	2.717	0.88
11	B51	2.75395	2.732	0.80
12	B52	2.76685	2.745	0.79

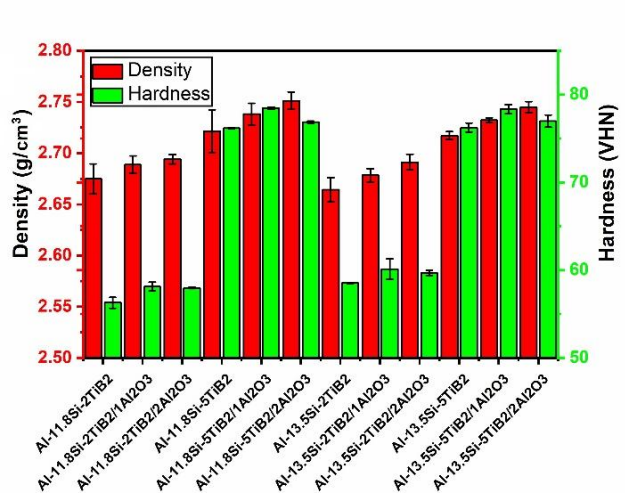

Figure 7. Density and hardness of composites as a function of Si and reinforcements

Figure 7 shows the variation in density values of the composites as a function of silicon content and reinforcements. It is evident that the advantage of lower density provided by silicon (2.33g/cm^3) and aluminium (2.7g/cm^3) has been offset by the reinforcements. A marginal increase in the density of the composites was noted as the quantity of Al_2O_3 (3.99 g/cm^3) and TiB_2 (4.52 g/cm^3) increased. However, it is also evident from Figure 7 that the hardness of these composites increases as the silicon content in the alloy rises. Hypereutectic alloy composites show higher hardness values as compared to hypo eutectic alloy composites. This is because the eutectic and primary silicon phases are harder than aluminum. An increasing number of harder phases improves the hardness of the composites. Further, an increase in TiB_2 content also increases the hardness of the composites. The synergetic effect of grain refinement by TiB_2 and the high hardness value of the ceramic itself are the main reasons for the improved hardness of the composites [25–27]. Though Al_2O_3 is capable of grain refinement, this effect is not significant beyond 1wt.% in the composites, as agglomeration begins to form at higher amounts of Al_2O_3. This is also reflected in the hardness values in Figure 7.

4. Conclusions

Conclusions drawn from this present study are as follows:

- Al-Si-TiB_2/Al_2O_3 hybrid composites were successfully synthesized via a stir casting route, following in-situ and ex-situ methods.
- In-situ formation of TiB_2 was confirmed by the XRD study.
- Marginal increase in density is observed in the composites with increasing amount of reinforcing ceramic particles, but a significant increase in hardness values is witnessed, though it has been restricted to 1 wt. % Al_2O_3.
- Both Al_2O_3 and TiB_2 are found to decrease the wear of the composites, but only up to 1wt. % Al_2O_3 is beneficial in this regard.
- Both the reinforcing particles are found responsible for grain refinement, but agglomeration starts when Al_2O_3 content exceeds 1 wt. %.

Acknowledgements

The authors acknowledge the support and access to laboratory facilities granted by the Department of Metallurgical and Materials Engineering, Indira Gandhi Institute of Technology, Sarang, Odisha-759146, India, NIT, Rourkela Odisha- 769008 and GCE, Keojhar, Odisha-758002.

Ethical issue

The authors are aware of and comply with best practices in publication ethics, specifically regarding authorship (avoidance of guest authorship), dual submission, manipulation of figures, competing interests, and compliance with research ethics policies. The authors adhere to publication requirements that the submitted work is original and has not been published elsewhere.

Data availability statement

The manuscript contains all the data. However, more data will be available upon request from the authors.

Conflict of interest

The authors declare no potential conflict of interest.

References

[1] Dasgupta R. Aluminium Alloy-Based Metal Matrix Composites: A Potential Material for Wear Resistant Applications. International Scholarly Research Notices 2012; 2012: e594573.

[2] Suresh S, Shenbag N, Moorthi V. Aluminium-Titanium Diboride (Al-TiB2) Metal Matrix Composites: Challenges and Opportunities. Procedia Engineering 2012; 38: 89–97.

[3] Committee AH. Properties and Selection: Nonferrous Alloys and Special-Purpose Materials. ASM International. Epub ahead of print 1 January 1990. DOI: 10.31399/asm.hb.v02.9781627081627.

[4] Natarajan S, Narayanasamy R, Kumaresh Babu SP, et al. Sliding wear behaviour of Al 6063/TiB2 in situ

composites at elevated temperatures. Materials & Design 2009; 30: 2521–2531.
[5] Mandal A, Murty BS, Chakraborty M. Wear behaviour of near eutectic Al–Si alloy reinforced with in-situ TiB2 particles. Materials Science and Engineering: A 2009; 506: 27–33.
[6] Yashpal, Sumankant, Jawalkar CS, et al. Fabrication of Aluminium Metal Matrix Composites with Particulate Reinforcement: A Review. Materials Today: Proceedings 2017; 4: 2927–2936.
[7] Mandal A, Maiti R, Chakraborty M, et al. Effect of TiB2 particles on aging response of Al–4Cu alloy. Materials Science and Engineering: A 2004; 386: 296–300.
[8] Sozhamannan GG, Prabu SB, Venkatagalapathy VSK. Effect of Processing Paramters on Metal Matrix Composites: Stir Casting Process. JSEMAT 2012; 02: 11–15.
[9] Sahoo SK, Majhi J, Patnaik SC, et al. Microstructure characterisation and dry sliding wear behaviour of Al-Si near eutectic and hypereutectic alloys reinforced with in-situ TiB2 synthesized by stir casting route. Springer Nature 2024; 4: 87.
[10] Sahoo JK, Sahoo SK, Sutar H, et al. Wear behavior of Al-Si alloy based metal matrix composite reinforced with TiB2. IOP Conf Ser: Mater Sci Eng 2017; 178: 012025.
[11] Sahoo SK, Sarangi B, Patnaik SC, et al. Studies on in-situ TiB2 reinforced Al-Si alloys synthesized by stir casting method. Materials Today: Proceedings 2020; 33: 5362–5367.
[12] Kori SA, Chandrashekharaiah TM. Studies on the dry sliding wear behaviour of hypoeutectic and eutectic Al–Si alloys. Wear 2007; 263: 745–755.
[13] Tjong SC, Wu SQ, Zhu HG. Wear behavior of in situ TiB2·Al2O3/Al and TiB2·Al2O3/Al–Cu composites. Composites Science and Technology 1999; 59: 1341–1347.
[14] El-Mahallawi I, Shash A, Amer A. Nanoreinforced Cast Al-Si Alloys with Al2O3, TiO2 and ZrO2 Nanoparticles. Metals 2015; 5: 802–821.
[15] Pramod SL, Bakshi SR, Murty BS. Aluminum-Based Cast In Situ Composites: A Review. J of Materi Eng and Perform 2015; 24: 2185–2207.
[16] PETRU MOLDOVAN1, , MIHAI BUTU1, , GABRIELA POPESCU1, et al. Thermodynamics of Interactions in Al-K2 TiF6-KBF4 System. Revista de Chimie 2010; 61: 828–832.
[17] Sun J, Zhang X, Zhang Y, et al. Modification mechanism of primary silicon by TiB2 particles in a TiB2/ZL109 composite. J Mater Sci 2015; 50: 1237–1247.
[18] Michael Rajan HB, Ramabalan S, Dinaharan I, et al. Effect of TiB2 content and temperature on sliding wear behavior of AA7075/TiB2 in situ aluminum cast composites. Archives of Civil and Mechanical Engineering 2014; 14: 72–79.
[19] Satish Kumar T, Thankachan T, Giri J, et al. Microstructural characterization of in-situ MgAl2O4 nanoparticles reinforced Al–2Mg–1Si composite produced using the ultrasonic assisted stir casting process. Journal of Materials Research and Technology 2024; 29: 2458–2467.
[20] Rafi SM, Satish Kumar T, Thankachan T, et al. Synergistic Effect of FSP and TiB2 on Mechanical and Tribological Behavior of AA2024 Surface Composites. Journal of Tribology 2023; 145: 114501.
[21] Puspitasari P, Sasongko MIN, Sukarni, et al. Mechanical properties of Al-Si alloy with nanoreinforced manganese oxide by stir casting method. Malang, Indonesia, p. 050003.
[22] Kumar TS, Thankachan T, Shalini S, et al. Microstructure, hardness and wear behavior of ZrC particle reinforced AZ31 surface composites synthesized via friction stir processing. Sci Rep 2023; 13: 20089.
[23] Dwivedi DK, Arjun TS, Thakur P, et al. Sliding wear and friction behaviour of Al–18% Si–0.5% Mg alloy. Journal of Materials Processing Technology 2004; 152: 323–328.
[24] Sahu A, Behera A. Semi-solid Processing and Tribological Characteristics of Al-Cu Alloy. Materials Today: Proceedings 2015; 2: 1175–1182.
[25] Munro RG. Material Properties of Titanium Diboride. J Res Natl Inst Stand Technol 2000; 105: 709–720.
[26] Connor N. Silicon - Strength - Hardness - Elasticity - Crystal Structure. Material Properties, https://material-properties.org/Silicon-properties-applications-price-production/ (2020, accessed 28 March 2024).
[27] Connor N. Aluminium - Strength - Hardness - Elasticity - Crystal Structure. Material Properties, https://material-properties.org/Aluminium-properties-applications-price-production/ (2020, accessed 28 March 2024).